A Murine Model of Robotic Training to Evaluate Skeletal Muscle Recovery after Injury

STEFANO LAI[1], ALESSANDRO PANARESE[1], ROSS LAWRENCE[2], MICHAEL L. BONINGER[2,3,4,5], SILVESTRO MICERA[1,6], and FABRISIA AMBROSIO[2,3,4]

[1]Scuola Superiore Sant'Anna, Translational Neural Engineering Area, The BioRobotics Institute, Pisa, ITALY; [2]Department of Physical Medicine and Rehabilitation, University of Pittsburgh, Pittsburgh, PA; [3]McGowan Institute for Regenerative Medicine, University of Pittsburgh Medical Center, University of Pittsburgh, Pittsburgh, PA; [4]Department of Bioengineering, University of Pittsburgh, Pittsburgh, PA; [5]Department of Rehabilitation Science and Technology, University of Pittsburgh, Pittsburgh, PA; and [6]Ecole Polytechnique Federale de Lausanne (EPFL), Bertarelli Foundation Chair in Translational NeuroEngineering Laboratory, Center for Neuroprosthetics and Institute of Bioengineering, Lausanne, SWITZERLAND

ABSTRACT

LAI, S., A. PANARESE, R. LAWRENCE, M. L. BONINGER, S. MICERA, and F. AMBROSIO. A Murine Model of Robotic Training to Evaluate Skeletal Muscle Recovery after Injury. *Med. Sci. Sports Exerc.*, Vol. 49, No. 4, pp. 840–847, 2017. **Purpose**: *In vivo* studies have suggested that motor exercise can improve muscle regeneration after injury. Nevertheless, preclinical investigations still lack reliable tools to monitor motor performance over time and to deliver optimal training protocols to maximize force recovery. Here, we evaluated the utility of a murine robotic platform (i) to detect early impairment and longitudinal recovery after acute skeletal muscle injury and (ii) to administer varying intensity training protocols to enhance forelimb motor performance. **Methods**: A custom-designed robotic platform was used to train mice to perform a forelimb retraction task. After an acute injury to bilateral biceps brachii muscles, animals performed a daily training protocol in the platform at high (HL) or low (LL) loading levels over the course of 3 wk. Control animals were not trained (NT). Motor performance was assessed by quantifying force, time, submovement count, and number of movement attempts to accomplish the task. Myofiber number and cross-sectional area at the injury site were quantified histologically. **Results**: Two days after injury, significant differences in the time, submovement count, number of movement attempts, and exerted force were observed in all mice, as compared with baseline values. Interestingly, the recovery time of muscle force production differed significantly between intervention groups, with HL group showing a significantly accelerated recovery. Three weeks after injury, all groups showed motor performance comparable with baseline values. Accordingly, there were no differences in the number of myofibers or average cross-sectional area among groups after 3 wk. **Conclusion**: Our findings demonstrate the utility of our custom-designed robotic device for the quantitative assessment of skeletal muscle function in preclinical murine studies. Moreover, we demonstrate that this device may be used to apply varying levels of resistance longitudinally as a means manipulate physiological muscle responses.
Key Words: SKELETAL MUSCLE INJURY, STRENGTH, ROBOTIC TRAINING, MOUSE, SKELETAL MUSCLE REGENERATION

Muscle injuries are common and represent one of the leading causes of motor dysfunction (15). Although skeletal muscles are able to regenerate spontaneously after damage, the healing process after a severe injury is often slow and functionally incomplete. Optimal clinical treatment remains unclear (6). As a result, significant efforts have been dedicated to the development of methods to enhance skeletal muscle recovery. Several studies have shown that mechanical loading and motor exercise can improve the efficacy of muscle regeneration (11,12,18). Indeed, exercise is capable of altering the behavior and the number of the myogenic precursors, i.e., satellite cells, responsible for myofiber hypertrophy and repair (4,19).

Mechanical stimulation through muscle loading alters both local and systemic levels of physiological factors, i.e., oxygen, growth factors, and cytokine concentrations. Satellite cells are located between the myofiber basal lamina and the plasma membrane in a normally quiescent state (29). In response to injury, satellite cells become activated, proliferate, and differentiate into myofibers. Most mechanistic studies investigating the cascade of events leading to muscle spontaneous regeneration have used mouse models (7). Such studies often involve *in vitro* preparations of isolated primary cells, histological analysis, or functional muscle analysis in anesthetized animals (such as neuromuscular electrical

Address for correspondence: Fabrisia Ambrosio, Ph.D, M.P.T., McGowan Institute for Regenerative Medicine, University of Pittsburgh Medical Center, University of Pittsburgh, Bridgeside Point Building II, Suite 308, 450 Technology Drive, Pittsburgh, PA 15219; E-mail: ambrosiof@upmc.edu.
S. M. and F. A. have equal contribution as senior scientists.
Submitted for publication March 2016.
Accepted for publication October 2016.
Supplemental digital content is available for this article. Direct URL citations appear in the printed text and are provided in the HTML and PDF versions of this article on the journal's Web site (www.acsm-msse.org).

0195-9131/17/4904-0840/0
MEDICINE & SCIENCE IN SPORTS & EXERCISE®

DOI: 10.1249/MSS.0000000000001160

stimulation or *in situ* contractile testing). Voluntary *in vivo* protocols, on the other hand, offer the important advantage of providing clinically relevant information on the ability of training regimens to enhance muscle recovery after injury. Several murine studies have investigated the ability of swimming (8), voluntary wheel running (5), or treadmill running to modulate muscle regeneration after injury (2,31). However, these motor exercises are not specific to the injured muscle. Moreover, these exercise regimens do not allow for a quantitative or longitudinal measures of force production in the muscle of interest. Although sensors and actuators have been used to quantify kinetic and kinematic parameters, the number of murine models of robotic training is still limited (38).

Here, we evaluate the utility of a novel robotic platform as a means of volitional forelimb muscle training in mice (38). In the context of muscle injury, this system presents important advantages over alternative protocols. First, it allows for the noninvasive and quantitative assessment of forelimb muscle function after injury and over time. Second, the intensity of the training task can be modified in a manner comparable with classic motor training, while maintaining high repeatability and accuracy. In the first part of this study, we determined the capability of the platform to detect strength impairment after an acute biceps injury. Next, we implemented a robot-based training protocol to investigate whether manipulation of loading resistance affects motor recovery.

METHODS

Animals

A total of 20 C57 BL/6 male mice (Jackson Laboratories, Bar Harbor, ME) were used. Animals were between 3 and 5 months of age and weighed 28 ± 5 g. Mice were housed in a room kept at 20°C–23°C and a 12-h light–12-h dark cycle. Animals had *ad libitum* access to water and standard chow. This study was performed in accordance with the recommendations in the Guide for the Care and Use of Laboratory animals of the National Institutes of Health. All experiments were approved by the Institutional Animal Care and Use Committee of University of Pittsburgh (authorization protocol no. IS00004640).

Robotic Platform

The animals were trained by means of a robotic platform, as we previously described (38). Briefly, the robotic system comprises a linear actuator, a six-axis load cell, a precision linear slide with an adjustable friction, and a custom-designed handle that was fastened to the left wrist of the mouse (Fig. 1A). This device has a resolution of 2.5 mN root mean square, in all directions and a bandwidth of 0–1.2 kHz (38). One end of the handle was screwed on the load cell for lossless transfer of the forces to the sensor, whereas the other end formed a support for the animal wrist. During the task, the animal was kept in a U-shaped restrainer and a post that was cemented to the skull stabilized the animal's head. The training session was divided into "trials," repeated sequentially and consisting of five steps. First, the linear motor pushed the handle and extended the mouse left forelimb by 10 mm (full upper extremity extension). Next, the motor quickly decoupled from the slide, and a tone lasting 0.5 s informed the mouse to initiation the task. If able, the animal voluntarily pulled the handle back (i.e., forelimb flexion back to the starting position). On successful completion of the task, a tone lasting 1 s was emitted. Finally, within a fixed time delay of 5 s, the animal was given access to a liquid reward, i.e., 10 μL of sweetened condensed milk, before starting a new cycle (see Video, Supplemental Digital Content 1, Representative task performed by an animal on the platform. The linear motor pushed the handle and extended the mouse left forelimb. Afterwards, the motor quickly moved back, allowing the animal to voluntarily pull back the handle up to the starting position, http://links.lww.com/MSS/A812).

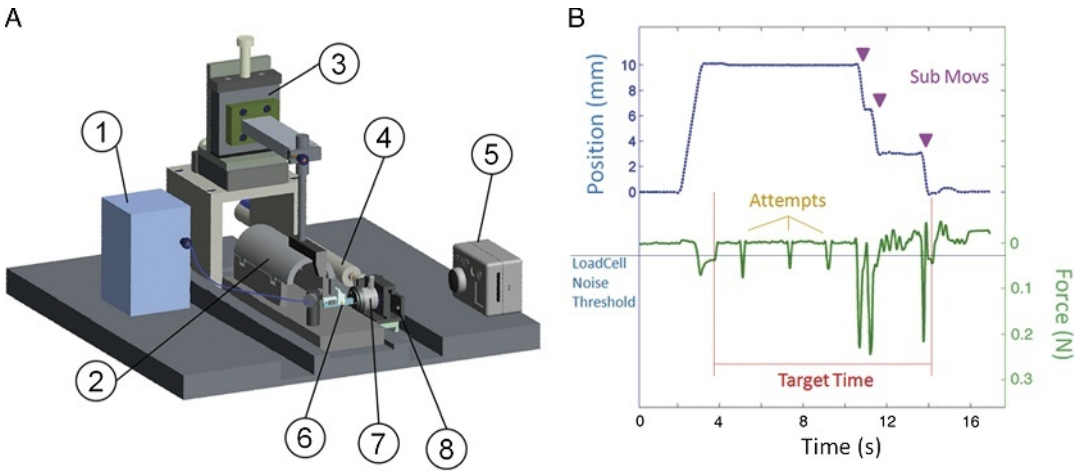

FIGURE 1—Robotic platform and parameters. A, Schematic of the robotic interface consisting of a peristaltic pump for reward delivery (1), mouse restrainer (2), micromanipulator (3), linear actuator (4), video camera (5), handle (6), load cell (7), slide (8). B, Computed parameters (i.e., target time, mean force, submovements [Sub Movs], and attempts) are shown during the performance of a representative task on the robot (F_s = 0.2 N).

The mouse must overcome a specified force threshold, i.e., static friction, F_s, to retract its forelimb and complete the task. To habituate the animals to the robotic device, mice in all groups were trained at an F_s of 0.2 N (see Chronic implant, shaping, and Preinjury Training section), whereas the F_s was varied during the postinjury training according to group (see Postinjury Training section). All of the experimental sessions were recorded by a video camera placed perpendicular to the anteroposterior axis of movement. Position and speed signals were subsequently extracted from the video recordings and synchronized with the force signals recorded by the load cell. From these kinematic and kinetic signals, a series of parameters were automatically computed to describe detailed motor performance on the platform, including (i) target time (i.e., the time spent by the animal to accomplish a single retraction task), (ii) submovements (i.e., the number of movements needed to complete the task), (iii) mean force (i.e., the average force value computed during submovements along the anteroposterior axis), and (iv) number of attempts to move the handle, with "attempts" defined as those instances that the force exerted was not sufficient to overcome the static friction (Fig. 1B). The computation and the statistical analysis of these parameters were performed using custom-made algorithms developed in Matlab (Mathworks, Natick, MA).

Chronic implant, shaping, and preinjury training. Mice were maintained anesthetized with 2% isoflurane (Abbott Laboratories, Chicago, IL) in 100% O_2 gas. A metal post (length, 8 mm; diameter, 2 mm; weight, 0.2 g) was placed in proximity of the bregma and fixed with dentistry cement (Metabond; Parkell Inc., Edgewood, NY). Two days after the surgery, the animals started a "shaping" phase, which lasted for 5 d. The purpose of the shaping phase was to habituate the mice (i) to remain in the test-chamber, (ii) to keep the wrist in the handle, and (iii) to associate the reward with task completion. After the shaping phase, animals in all experimental groups started a preinjury training on the platform, which involved 10 trials per day for 5 d at F_s = 0.2 N.

Muscle injury. After preinjury training on the platform, all 20 animals underwent an injury to bilateral biceps. Mice were anesthetized with 2% isoflurane (Abbott Laboratories) in 100% O_2 gas. The hair was shaved, and the skin was cleaned with isopropyl alcohol. The position of the biceps was detected using the elbow as a landmark while inducing passive flexion and extension movements of the muscle. Cardiotoxin, CTX, from *Naja mossambica mossambica* venom (C9759, Sigma-Aldrich, St. Louis, MO) was suspended in phosphate-buffered saline (PBS) at a concentration of 1 $\mu g \cdot \mu L^{-1}$. Ten microliters of CTX was injected into the mid-belly region of bilateral biceps to induce an acute muscle injury. After injury, animals received a subcutaneous injection of an analgesic (5 $mg \cdot kg^{-1}$ Ketoralac). A second dose of Ketoralac was administered to all animals 24 h after injury.

Postinjury training. Two days after injury, animals were randomly assigned to one of three different groups: two groups performed a repetitive and daily task in the robotic platform at a high (HL, n = 6 mice) or low loading intensity (LL, n = 5 mice), whereas the third group was not trained (NT, n = 9 mice). Animals included in the HL and LL groups performed 10 trials per day, 4 $d \cdot wk^{-1}$ for 3 wk, at an F_s of 0.3 N or 0.1 N, respectively. These F_s values were selected according to the average maximal force-producing capacity (MFC) of the animals 2 d after muscle injury. MFC ranged between 0.31 and 0.60 N, and the average value computed on all of the mice tested was 0.40 ± 0.06 N. Thus, 0.3 and 0.1 N corresponded to 75% and 25% of MFC, respectively. Furthermore, to compare force recovery across the three groups, animals were tested on the platform once a week, at a loading intensity of F_s = 0.2 N, the same friction used for the prelesion training.

Histological Analysis

All the animals were euthanized 24 d after the CTX injection. To evaluate the extent of muscle injury across groups, biceps muscles were harvested and immediately fixed in 2% glutaraldehyde for 2 h. The muscles were then immersed in 30% sucrose for 24 h, and the solution was refreshed every 8 h. The biceps muscles were then frozen in liquid nitrogen-cooled 2-methyl-butane and subsequently sectioned through its entirety (Cryotome FSE Cyrostat, Thermo Scientific, Pittsburgh, PA) into 10 μm slices. Immunofluorescent labeling for laminin was performed to quantify the total number of myofibers, the myofiber cross-sectional area (CSA), and the regeneration index (RI). The RI is defined as (2)

$$\mathrm{RI} = \frac{\text{total number of fibers with centrally located nuclei}}{\text{total number of fibers}} \times 100.$$

Any muscle fiber with cytoplasm between the nucleus and the myofiber periphery was considered to be "centrally nucleated." The slides were fixed for 15 min at room temperature (RT) in 2% paraformaldehyde and then washed with 1× PBS three times. Samples were then treated with 0.03% Triton X-100 (Fluka, Switzerland) for 15 min at RT. Slides were then washed three times with PBS and placed to dry for 2 min on a paper towel at RT. Each slide was coated with primary rabbit antibodies to laminin (ab 11576; Abcam) at a dilution of 1:200 in 3% goat serum (A11006; Jackson Immuno Research, West Grove, PA) at RT for 1 h. Slides were then washed three times with PBS and coated with goat anti-rabbit 488 (A-11006; Life Technologies, Grand Island, NY) at a dilution of 1:400 diluted in 3% goat serum for 40 min in a dark room. Finally, the slides were thoroughly washed with PBS three times and mounted with coverslip using DAPI mounting media (DAPI Fluromount-G, Life Technologies). The slides were left to dry at 4°C overnight before imaging.

Slides were imaged using a Nikon Eclipse 90i bright field microscope (Nikon, Japan). The Nikon Elements AR (Nikon) was used to set a threshold providing a binary representation of each image, and the number of myofibers and the CSA were calculated for each image. A total of three images per sample were analyzed by an investigator who was blinded to the animal grouping.

Statistical Analysis

Data were analyzed by using SigmaPlot 11.0 software (Systat Software Inc., San Jose, CA), Matlab (Mathworks), and the free software statistical environment "R" (34), considering the value of significance at $\alpha = 0.05$. The Lilliefors test was used to assess the normality of the baseline values. To estimate differences in longitudinal variation among groups, a two-way repeated-measures ANOVA was performed. When there was no significant group–time interaction, a one-way repeated-measures ANOVA was used to assess longitudinal changes. Tukey's *post hoc* method was then used for pairwise comparisons. A one-way ANOVA was also used to compare the number of myofibers, the CSA, and the RI among groups. A linear regression model, followed by a residual analysis and Shapiro–Wilk test, was used to describe the time course of the parameters after lesion in HL and LL groups.

RESULTS

Upon completion of the initial training, all of the animals showed stable performance in all of the motor parameters, and the values collected over the last 3 d of training followed a Gaussian distribution (Lilliefors test, $P > 0.5$ for each parameter). For each animal, the baseline values of the parameter X collected for 3 d were pooled together to compute a unique baseline value B_x, with X = target time, submovements, mean force, or number of attempts.

Injury resulted in a significant reduction in the force exerted by the forelimb after 2 d, regardless of the training group (Fig. 2B; comparison *B* vs day 2, $P < 0.001$ in HL, $P = 0.001$ in LL, $P = 0.004$ in NT). In the subsequent weeks after injury, mean force eventually returned to baseline values. Although there was no significant group–time interaction when considering the other parameters ($P = 0.170$, 0.702, and 0.877, for target time, submovements, and attempts, respectively), the interaction was significant when considering mean force ($P = 0.007$), and the recovery time of muscle force production was inversely correlated with loading level. Animals in HL recovered significantly faster than the other two groups, i.e., within 9 d after injury, when compared with their own baseline levels (Fig. 2B; $P = 0.024$ compared with LL and $P < 0.001$ compared with NT). Significant differences were also observed between HL versus LL (comparison at day 9, $P < 0.033$) and HL versus NT (comparison at day 9, $P < 0.005$). Animals in LL recovered to baseline values in the following week, whereas animals in NT group did not return to baseline performance level until 3 wk after injury.

After the injury, target time showed significant variation over time (Fig. 2A; $P = 0.012$ in HL, $P < 0.001$ in LL, $P < 0.001$ in NT). As expected, this parameter was significantly increased after lesion in all groups (comparison *B* vs day 2, $P = 0.03$ in HL, $P = 0.005$ in LL, $P < 0.001$ in NT). Importantly, movement production was also impaired after damage (Fig. 2D; $P = 0.033$ in HL, $P = 0.003$ in LL, $P = 0.003$ in NT), as evidenced by a consistent increase in the number of attempts (comparison *B* vs day 2, $P = 0.04$ in HL, $P = 0.01$ in LL, $P < 0.001$ in NT). Target time and number of attempts returned to baseline values within 9 d from the injury. On the other hand, there was no difference in the number of submovements required to complete the task in any of the three training groups (Fig. 2C; $P > 0.690$ in HL, $P > 0.181$ in LL, $P = 0.409$ in NT), suggesting that motor coordination might be only slightly affected.

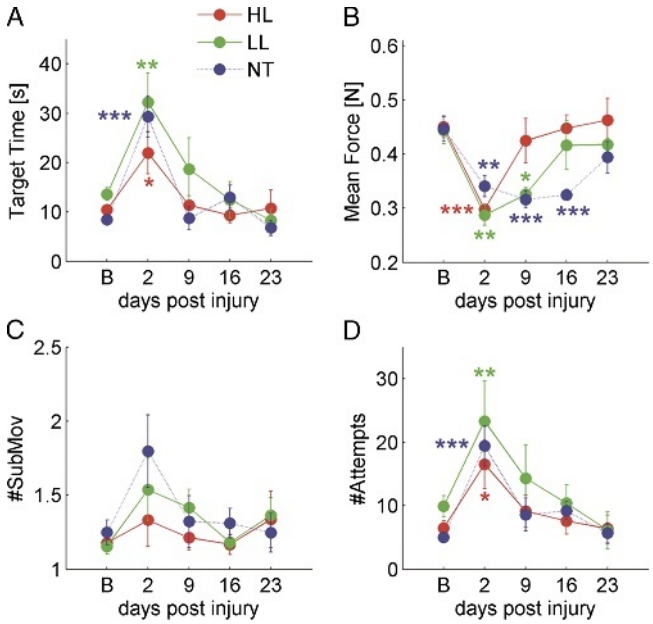

FIGURE 2—Postinjury comparison. Target time (A), mean force (B), submovements (C), and attempts (D) at the assessment days of the protocol (friction force $F_s = 0.2$ N) for the not trained group (NT, *blue*), high loading group (HL, *red*), and low loading group (LL, *green*). Data are mean ± SE. B indicates prelesion baseline. Two-way repeated-measures ANOVA, followed by Tukey's *post hoc* test, for the mean force parameter (B). One-way repeated-measures ANOVA, followed by Tukey's *post hoc* test, for the other three parameters in each group. *$P < 0.05$; **$P < 0.01$; ***$P < 0.001$. The stars refer to a comparison with the same group's baseline values.

For each parameter, a linear time evolution model was fitted to the data from all of the postinjury sessions performed by animals in HL and LL separately. Compared with the other parameters, the mean force in HL showed the strongest accordance with a linear model of time evolution throughout the training ($r = 0.71$, $P < 0.001$ for mean force in HL, vs $r < 0.6$, $P < 0.001$ for LL and NT). The goodness of the linear model on fitting the mean force in HL was investigated further and ultimately confirmed by the Shapiro–Wilk test ($P = 0.8$; Fig. 3B, *dashed line*).

Consistent with findings demonstrating no difference in the force-producing capacity of muscles across the three treatment groups after 3 wk, there were no differences among the three groups when comparing the number of myofibers ($P = 0.414$) or the CSA ($P = 0.376$), Table 1. Although force-producing capacity returned to baseline values after 3 wk, histological analysis revealed ongoing regeneration, as determined by the presence of centrally

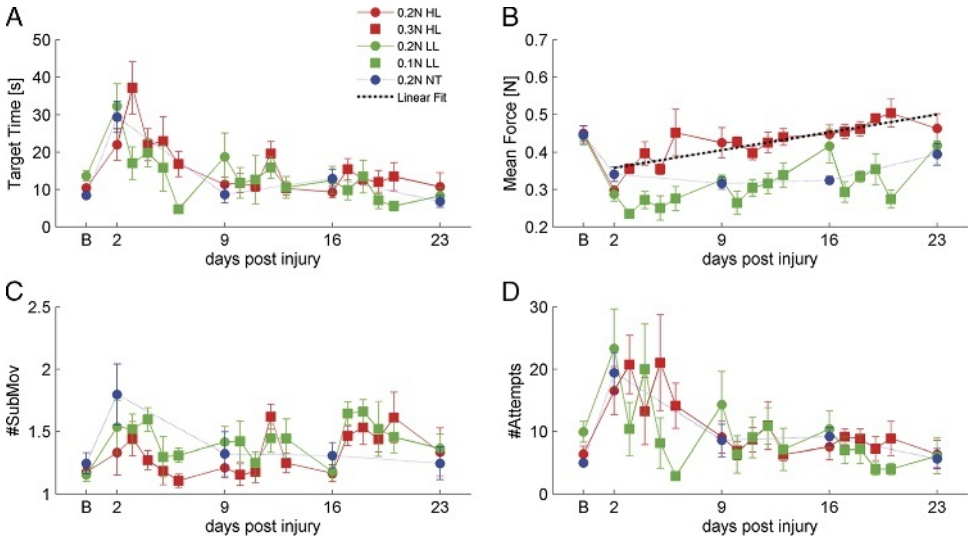

FIGURE 3—Postinjury time course of the performance on the platform. Postlesion time course of target time (A), mean force (B), submovements (C), and attempts (D) for the not trained group (NT, *blue*), high loading group (HL, *red*), and low loading group (LL, *green*). The round markers correspond to the assessment days, i.e., sessions with friction force F_s = 0.2 N, whereas the square markers coincide with the training days, i.e., sessions with F_s = 0.3 N and F_s = 0.1 N for HL and LL, respectively. The *dashed line* on the panel B is the linear model, which best fits the red curve (r = 0.71, P < 0.001). Data are presented as mean ± SE. B indicates prelesion baseline.

nucleated fibers in all groups (Fig. 4). However, there was no difference in the RI across the three groups (P = 0.114), Table 1.

DISCUSSION

In this article, we evaluated the utility of a robotic platform to noninvasively and longitudinally test voluntary muscle function after an acute skeletal muscle injury. In addition, we evaluated the ability of this device to serve as a rehabilitation platform with the capability of administering a range of training protocols. Findings suggest that the system is sensitive enough to detect deficits in forelimb movements after a local injury of the biceps and that it allows for distinction of functional improvements according to varying loading intensities.

Although not specifically measured, the forelimb retraction task used in this system is presumably specific to action of the proximal forelimb muscles, while largely excluding activity of the elbow extensors (*triceps*) and the distal forelimb (forepaw and digit muscle groups) (38). The motion required by the robotic device is comparable with the planar forelimb retraction phase of a skilled reaching task, a well-known test in which animals are trained to reach for food pellets with their forepaw and to bring the pellet to their mouth (26). The retraction phase of this task requires elbow flexion and a shoulder extension, achieved by activation of the biceps and the shoulder extensors (in particular the spinodeltoideus), respectively (23). Although our study lacks direct evidence of biceps activation, 2 d after a localized CTX-induced injury to the biceps, performance impairment was evidenced by significant variations in the task duration, exerted force, and number of movement attempts with respect to baseline (Fig. 2A, B, D, *B* vs day 2), suggesting forelimb flexor involvement for the retraction task. There was also a slight, but not significant, increase in the number of submovements after 2 d (Fig. 2C). The number of submovements is typically used to quantify movement smoothness poststroke, both in humans (22,32) and mice (27), and is related to movement coordination abilities (35). All mice in the study retained the ability to accomplish the forelimb retraction task after injury, although performance was impaired. Because CTX preserves the basal lamina sheaths surrounding the original muscle fibers (10), thought to be the crucial factor in determining the success of innervation of regenerated muscles (37), motor end plate (and thus motor unit recruitment) is only partially affected by this type of injury. The preserved motor ability in performing the task is thus mostly likely due to some residual action of the biceps, together with the continuous synergistic action of the brachialis and deltoid.

In all groups, time target and number of attempts returned to baseline values 9 d after injury (Fig. 2A and D). Although all mice were able to overcome the force threshold (0.2 N in the assessment sessions), only the HL group's performance was similar to baseline values at 9 d postinjury. The animals in this group were required to exert a higher force (0.3 N) to successfully perform the task, making the task considerably

TABLE 1. Histological analysis.

	NT	LL	HL
No. myofibers (fibers/field of view)	413 ± 69	463 ± 108	394 ± 37
CSA (μm^2)	626 ± 163	492 ± 139	571 ± 69
RI (%)	79.29 ± 2.96	70.91 ± 19.62	68.54 ± 12.32

Number of myofibers, CSA, and RI mean ± SE values 24 d after lesions are reported for the NT, LL, and HL groups.

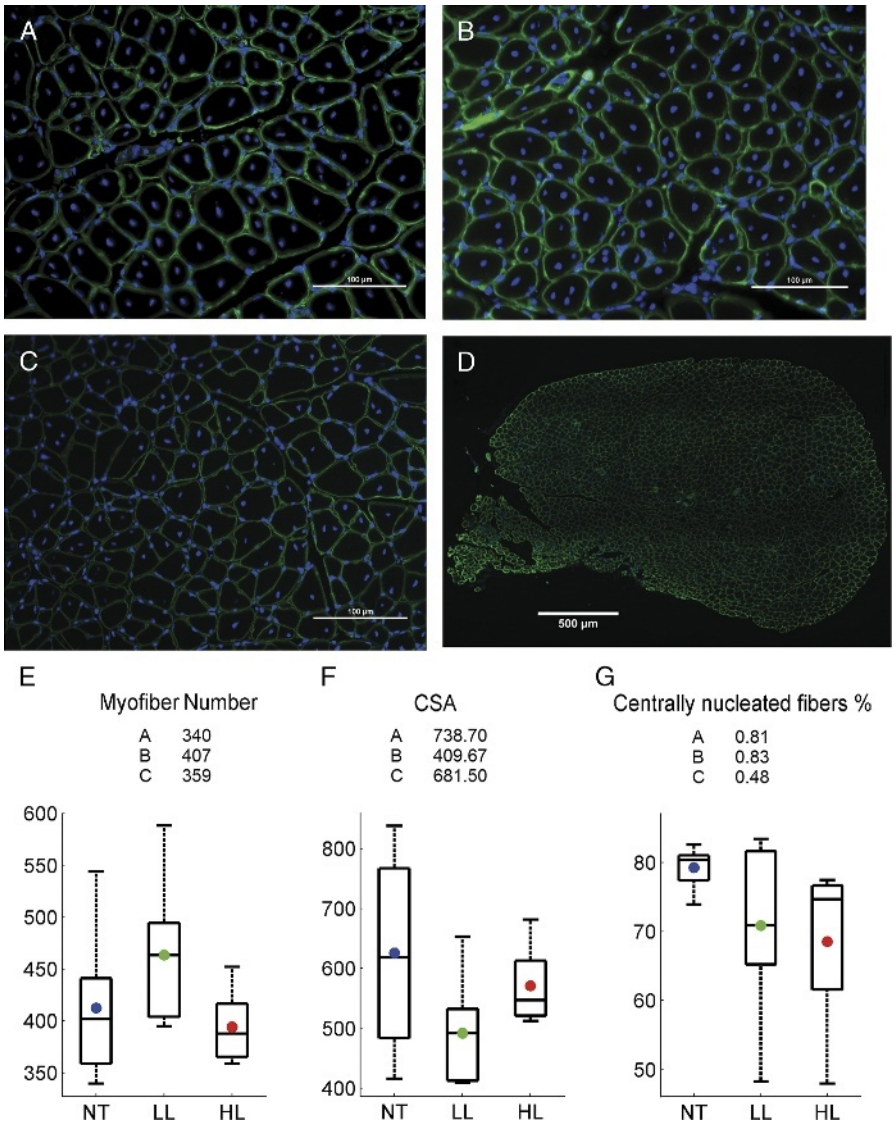

FIGURE 4—Muscle histology. Representative laminin stain of a biceps muscle section of the NT (A), LL (B), and HL (C) groups (laminin, *green*; DAPI (nuclei), *blue*; magnification, ×20; scale bar = 100 µm). D, Representative view of a whole slice collected from the biceps of an animal of HL group (magnification, ×1; scale bar = 500 µm). E, Myofiber number from the A–B–C muscle sections (*top*) and the distribution of the myofiber number values among the three groups (box plots on the *bottom*). F, CSA from the A–B–C muscle sections (*top*) and the distribution of the CSA values for the three groups (box plots on the *bottom*) are reported. Centrally nucleated fibers percentage from the A–B–C muscle sections (*top*) and the distribution of the centrally nucleated fibers percentage (box plots on the *bottom*) among the three groups are shown on panel G. Round colored markers on the box plots point out the average values of the distributions.

more difficult when compared with the other groups. This is further evidenced by the increased target time and number of attempts in the first week of training when compared with the other groups (Fig. 3A, D).

The application of mechanical stimulation to promote tissue regeneration is a mainstay of physical therapy practice. This concept is not new, and "mechanotherapy" was first defined in the late 19th century as "the employment of mechanical means for the cure of disease" (24). Skeletal muscle is particularly amenable to the beneficial effects of mechanical stimulation, as muscle loading has been shown to stimulate growth factor secretion and angiogenesis (9,16,17) as well as muscle stem (satellite) cell activation (20,33). In fact, several studies have demonstrated the ability of exercise to increase satellite cell numbers in uninjured skeletal muscle (3,18,21) and to promote the fibers regeneration after injury. Khattak et al. (25) found that the number of myotubes of injured gastrocnemius was increased in rats performing a sustained exercise on the running wheel when compared with immobilized animals. Moreover, Ambrosio et al. (2) showed that intensive treadmill running significantly increased the myogenic potential and migration of muscle progenitors transplanted into severely injured tibialis anterior muscles. Similarly, Bouchentouf et al. (8) observed that an intense swimming task can enhance myoblast transplantation in injured tibialis anterior muscle of dystrophin deficient (*mdx*) mice. Overall, these studies suggest exercise has the potential to enhance skeletal muscle recovery. However,

major gaps in the identification of optimal muscle loading protocols to maximize force recovery over time remain.

The results presented in this work suggest that recovery after muscle injury may be accelerated by a motor exercise with high resistance loading. We limited the number of trials to 10 per session to minimize the potential adverse effects of muscle fatigue. Interestingly, the time course of the force production in the HL group (Fig. 3B) reveals a continuous linear increase of the performance during training. On the other hand, force production in the LL group returned to baseline values only after 16 d (Fig. 2B), suggesting that the lower resistance load (0.1 N; approximately 25% of the MFC) was less effective in promoting strength recovery after an acute injury.

Because the animals were immobilized on the platform, we cannot rule out the possibility that stress may have affected muscle regeneration. So as to minimize variability resulting from stress, all animals were exposed to the apparatus for the same amount of time during the habituation phase. Moreover, throughout testing, the level of stress was continuously monitored by the experimenter by evaluating the motivation of the animals during each session of exercise. If the animal ceased to accept the liquid reward (i.e., the animal stopped licking the milk drop from the gavage needle), the session was immediately terminated. This was only observed in <5% of the cases over the course of the experiment.

Consistent with findings demonstrating that all groups returned to similar force-producing capacity after 3 wk, histological analysis at this same time point revealed ongoing regeneration that was comparable across all three groups. Although no statistical differences were observed according to a one-way ANOVA, a *t*-test comparison of the RI between HL (68.54% ± 12.32%) and NT (79.29% ± 2.96%) groups suggests that high-intensity training may be associated with a decrease in active regeneration ($P = 0.03$) and, potentially, an accelerated regeneration process. An increase in muscular strength without noticeable hypertrophy may also suggest a neural involvement in the generation of muscular strength (14). In clinical studies, the role of neural involvement is suggested to be particularly important during the early phase of strength training (14), whereas muscle hypertrophy may still be absent several weeks after initiation of the training regimen (1). As such, neuromuscular adaptation across experimental groups may also be a contributing factor in these studies.

The biceps muscles show some anatomical differences when comparing mice and humans, especially in terms of fiber composition and myosin isoforms (28,39). Moreover, the biceps contribute to weight bearing, stabilization, and ambulation in quadrupedal animals such as mice (30). However, this muscle also shares important functional similarities between the two species (e.g., for reaching and holding food) (13,36).

Taken together, our results demonstrate the utility of this robotic platform to both characterize motor deficits after an acute muscle injury and monitor longitudinal force recovery. As such, this device may also be useful for future studies investigating the mechanistic basis underlying functional skeletal muscle recovery. The current findings may also help to inform translational studies and suggest that a specific and high-load training protocol may accelerate spontaneous recovery after local damage, as compared with a low-intensity protocol or no treatment. Finally, these findings may inform future studies aimed at investigating disease progression in other models of muscle dysfunction, such as muscular dystrophy, and may help develop and refine robotic training protocols to improve skeletal muscle function and regeneration after injury.

The authors declared no potential conflicts of interest with respect to the research, authorship, and/or publication of this article.

This work was supported by funding from Fondazione Pisa, Italy, and the University of Pittsburgh Medical Center Rehabilitation Institute, Pittsburgh, PA. The authors thank Ricardo Ferrari, PhD, PT, for his help in preparing and performing muscle injuries and Dr. Alessio Ghionzoli for his technical support in the setup of the robotic platform.

F. A., S. M., and M. L. B. designed the study; S. L. performed animal experiments; S. L. and A. P. performed data analysis; R. L. performed imaging and image quantification; and S. L., S. M., F. A., A. P., and R. L. wrote the article. All authors have read and approved the final version of the article. The results of the present study do not constitute endorsement by the American College of Sports Medicine.

REFERENCES

1. Akima H, Takahashi H, Kuno SY, et al. Early phase adaptations of muscle use and strength to isokinetic training. *Med Sci Sport Exerc*. 1999;31(4):588–94.
2. Ambrosio F, Ferrari RJ, Distefano G, et al. The synergistic effect of treadmill running on stem-cell transplantation to heal injured skeletal muscle. *Tissue Eng Part A*. 2010;16(3):839–49.
3. Ambrosio F, Kadi F, Lexell J, Fitzgerald GK, Boninger ML, Huard J. The effect of muscle loading on skeletal muscle regenerative potential: an update of current research findings relating to aging and neuromuscular pathology. *Am J Phys Med Rehabil*. 2009;88(2):145–55.
4. Ambrosio F, Tarabishy A, Kadi F, Brown EH, Sowa G. Biological basis of exercise-based treatments for musculoskeletal conditions. *PM R*. 2011;3(6 Suppl 1):S59–63.
5. Baltgalvis KA, Call JA, Cochrane GD, Laker RC, Yan Z, Lowe D. Exercise training improves plantar flexor muscle function in mdx mice. *Med Sci Sport Exerc*. 2012;44(9):1671–9.
6. Baoge L, Van Den Steen E, Rimbaut S, et al. Treatment of skeletal muscle injury: a review. *ISRN Orthop*. 2012;2012:689012.
7. Boldrin L, Muntoni F, Morgan JE. Are human and mouse satellite cells really the same? *J Histochem Cytochem*. 2010;58(11):941–55.
8. Bouchentouf M, Benabdallah BF, Mills P, Tremblay JP. Exercise improves the success of myoblast transplantation in mdx mice. *Neuromuscul Disord*. 2006;16(8):518–29.
9. Coggan AR, Spina RJ, King DS, et al. Skeletal muscle adaptations to endurance training in 60- to 70-yr-old men and women. *J Appl Physiol (1985)*. 1992;72(5):1780–6.
10. Couteaux R, Mira JC, d'Albis A. Regeneration of muscles after cardiotoxin injury. I. Cytological aspects. *Biol Cell*. 1988;62:171–82.
11. Crameri RM, Langberg H, Magnusson P, et al. Changes in satellite cells in human skeletal muscle after a single bout of high intensity exercise. *J Physiol*. 2004;558(Pt 1):333–40.

12. Dreyer HC, Blanco CE, Sattler FR, Schroeder ET, Wiswell RA. Satellite cell numbers in young and older men 24 hours after eccentric exercise. *Muscle Nerve*. 2006;33(2):242–53.
13. Fuentes I, Cobos AR, Segade LA. Muscle fibre types and their distribution in the biceps and triceps brachii of the rat and rabbit. *J Anat*. 1998;192(Pt 2):203–10.
14. Gabriel DA, Kamen G, Frost G. Neural adaptations to resistive exercise: mechanisms and recommendations for training practices. *Sport Med*. 2006;36(2):133–49.
15. Garrett WE Jr. Muscle strain injuries: clinical and basic aspects. *Med Sci Sports Exerc*. 1990;22(4):436–43.
16. Hepple RT, Mackinnon SL, Thomas SG, Goodman JM, Plyley MJ. Quantitating the capillary supply and the response to resistance training in older men. *Pflugers Arch*. 1997;433(3): 238–44.
17. Järvinen TA, Järvinen M, Kalimo H. Regeneration of injured skeletal muscle after the injury. *Muscles Ligaments Tendons J*. 2013;3(4):337–45.
18. Kadi F, Charifi N, Denis C, et al. The behaviour of satellite cells in response to exercise: what have we learned from human studies? *Pflugers Arch*. 2005;451(2):319–27.
19. Kadi F, Ponsot E. The biology of satellite cells and telomeres in human skeletal muscle: effects of aging and physical activity. *Scand J Med Sci Sport*. 2010;20(1):39–48.
20. Kadi F, Schjerling P, Andersen LL, et al. The effects of heavy resistance training and detraining on satellite cells in human skeletal muscles. *J Physiol*. 2004;558(Pt 3):1005–12.
21. Kadi F, Thornell LE. Concomitant increases in myonuclear and satellite cell content in female trapezius muscle following strength training. *Histochem Cell Biol*. 2000;113(2):99–103.
22. Kahn LE, Zygman ML, Rymer WZ, Reinkensmeyer DJ. Effect of robot-assisted and unassisted exercise on functional reaching in chronic hemiparesis. *Conference Proceedings of the 23rd Annual International Conference of the IEEE Engineering in Medicine and Biology Society*. 2001;2:1344–7.
23. Kanchiku T, Lynskey JV, Protas D, Abbas JJ, Jung R. Neuromuscular electrical stimulation induced forelimb movement in a rodent model. *J Neurosci Methods*. 2008;167(2):317–26.
24. Khan KM, Scott A. Mechanotherapy: how physical therapists' prescription of exercise promotes tissue repair. *Br J Sports Med*. 2009;43(4):247–52.
25. Khattak MJ, Ahmad T, Rehman R, Umer M, Hasan SH, Ahmed M. Muscle healing and nerve regeneration in a muscle contusion model in the rat. *J Bone Joint Surg Br*. 2010;92(6):894–9.
26. Klein A, Dunnett SB. Analysis of skilled forelimb movement in rats: the single pellet reaching test and staircase test. *Curr Protoc Neurosci*. 2012; doi: 10.1002/0471142301.ns0828s58.
27. Lai S, Panarese A, Spalletti C, et al. Quantitative kinematic characterization of reaching impairments in mice after a stroke. *Neurorehabil Neural Repair*. 2015;29:382–92.
28. Mathewson MA, Chapman MA, Hentzen ER, Fridén J, Lieber RL. Anatomical, architectural, and biochemical diversity of the murine forelimb muscles. *J Anat*. 2012;221(5):443–51.
29. Mauro A. Satellite cell of skeletal muscle fibers. *J Biophys Biochem Cytol*. 1961;9(2):493–5.
30. Naito A. Electrophysiological studies of muscles in the human upper limb: the biceps brachii. *Anat Sci Int*. 2004;79(1):11–20.
31. Palermo AT, LaBarge MA, Doyonnas R, Pomerantz J, Blau HM. Bone marrow contribution to skeletal muscle: a physiological response to stress. *Dev Biol*. 2005;279(2):336–44.
32. Panarese A, Colombo R, Sterpi I, Pisano F, Micera S. Tracking motor improvement at the subtask level during robot-aided neurorehabilitation of stroke patients. *Neurorehabil Neural Repair*. 2012;26:822–33.
33. Pietrangelo T, Di Filippo ES, Mancinelli R, et al. Low intensity exercise training improves skeletal muscle regeneration potential. *Front Physiol*. 2015;6:399.
34. R Development Core Team. *R: A Language and Environment for Statistical Computing*; 2008.
35. Rohrer B, Fasoli S, Krebs HI, et al. Movement smoothness changes during stroke recovery. *J Neurosci*. 2002;22(18):8297–304.
36. Sacrey LA, Alaverdashvili M, Whishaw IQ. Similar hand shaping in reaching-for-food (skilled reaching) in rats and humans provides evidence of homology in release, collection, and manipulation movements. *Behav Brain Res*. 2009;204(1):153–61.
37. Schiaffino S, Partridge T. *Skeletal Muscle Repair and Regeneration*. 2013.
38. Spalletti C, Lai S, Mainardi M, et al. A robotic system for quantitative assessment and poststroke training of forelimb retraction in mice. *Neurorehabil Neural Repair*. 2013;28(2):188–96.
39. Tirrell TF, Cook MS, Carr JA, Lin E, Ward SR, Lieber RL. Human skeletal muscle biochemical diversity. *J Exp Biol*. 2012;215(Pt 15): 2551–9.